EUROPEAN LABORATORY FOR PARTICLE PHYSICS

CERN–PPE/97–111
13 August 1997

Measurement of the b baryon lifetime and branching fractions in Z decays

The ALEPH Collaboration*

Abstract

Using approximately 4 million hadronic Z decays recorded with the ALEPH detector from 1991 through 1995, the lifetime of the b baryon is measured with three independent methods. From the impact parameter distribution of candidate leptons in 1063 events with $\Lambda\ell^-$combinations, the average b baryon lifetime is measured to be $1.20 \pm 0.08 \pm 0.06$ ps. From a sample of 193 fully reconstructed Λ_c^+ candidates correlated with a lepton and a sample of 46 $\Lambda\ell^+\ell^-$ combinations, the Λ_b lifetime is measured to be 1.21 ± 0.11 ps. The product branching fractions to these final states are $\mathrm{Br}(b \to \Lambda_b) \cdot \mathrm{Br}(\Lambda_b \to \Lambda\ell^-\overline{\nu}X) = 0.326 \pm 0.016 \pm 0.039\,\%$ for the first sample and $\mathrm{Br}(b \to \Lambda_b) \cdot \mathrm{Br}(\Lambda_b \to \Lambda_c^+\ell^-\overline{\nu}X) = 0.86 \pm 0.07 \pm 0.14\,\%$ for the second and third samples combined.

(Submitted to Zeitschrift für Physik)

* See the following pages for the list of authors.

The ALEPH Collaboration

R. Barate, D. Buskulic, D. Decamp, P. Ghez, C. Goy, J.-P. Lees, A. Lucotte, M.-N. Minard, J.-Y. Nief, B. Pietrzyk

Laboratoire de Physique des Particules (LAPP), IN^{2}P^3-CNRS, 74019 Annecy-le-Vieux Cedex, France

M.P. Casado, M. Chmeissani, P. Comas, J.M. Crespo, M. Delfino, E. Fernandez, M. Fernandez-Bosman, Ll. Garrido,[15] A. Juste, M. Martinez, G. Merino, R. Miquel, Ll.M. Mir, C. Padilla, I.C. Park, A. Pascual, J.A. Perlas, I. Riu, F. Sanchez

Institut de Física d'Altes Energies, Universitat Autònoma de Barcelona, 08193 Bellaterra (Barcelona), Spain[7]

A. Colaleo, D. Creanza, M. de Palma, G. Gelao, G. Iaselli, G. Maggi, M. Maggi, N. Marinelli, S. Nuzzo, A. Ranieri, G. Raso, F. Ruggieri, G. Selvaggi, L. Silvestris, P. Tempesta, A. Tricomi,[3] G. Zito

Dipartimento di Fisica, INFN Sezione di Bari, 70126 Bari, Italy

X. Huang, J. Lin, Q. Ouyang, T. Wang, Y. Xie, R. Xu, S. Xue, J. Zhang, L. Zhang, W. Zhao

Institute of High-Energy Physics, Academia Sinica, Beijing, The People's Republic of China[8]

D. Abbaneo, R. Alemany, U. Becker, A.O. Bazarko,[20] P. Bright-Thomas, M. Cattaneo, F. Cerutti, G. Dissertori, H. Drevermann, R.W. Forty, M. Frank, R. Hagelberg, J.B. Hansen, J. Harvey, P. Janot, B. Jost, E. Kneringer, J. Knobloch, I. Lehraus, P. Mato, A. Minten, L. Moneta, A. Pacheco, J.-F. Pusztaszeri,[23] F. Ranjard, G. Rizzo, L. Rolandi, D. Rousseau, D. Schlatter, M. Schmitt, O. Schneider, W. Tejessy, F. Teubert, I.R. Tomalin, H. Wachsmuth, A. Wagner[24]

European Laboratory for Particle Physics (CERN), 1211 Geneva 23, Switzerland

Z. Ajaltouni, A. Barrès, C. Boyer, A. Falvard, C. Ferdi, P. Gay, C . Guicheney, P. Henrard, J. Jousset, B. Michel, S. Monteil, J-C. Montret, D. Pallin, P. Perret, F. Podlyski, J. Proriol, P. Rosnet, J.-M. Rossignol

Laboratoire de Physique Corpusculaire, Université Blaise Pascal, IN^{2}P^3-CNRS, Clermont-Ferrand, 63177 Aubière, France

T. Fearnley, J.D. Hansen, J.R. Hansen, P.H. Hansen, B.S. Nilsson, B. Rensch, A. Wäänänen

Niels Bohr Institute, 2100 Copenhagen, Denmark[9]

G. Daskalakis, A. Kyriakis, C. Markou, E. Simopoulou, I. Siotis, A. Vayaki

Nuclear Research Center Demokritos (NRCD), Athens, Greece

A. Blondel, G. Bonneaud, J.C. Brient, P. Bourdon, A. Rougé, M. Rumpf, A. Valassi,[6] M. Verderi, H. Videau

Laboratoire de Physique Nucléaire et des Hautes Energies, Ecole Polytechnique, IN^{2}P^3-CNRS, 91128 Palaiseau Cedex, France

D.J. Candlin, M.I. Parsons

Department of Physics, University of Edinburgh, Edinburgh EH9 3JZ, United Kingdom[10]

E. Focardi, G. Parrini, K. Zachariadou

Dipartimento di Fisica, Università di Firenze, INFN Sezione di Firenze, 50125 Firenze, Italy

M. Corden, C. Georgiopoulos, D.E. Jaffe

Supercomputer Computations Research Institute, Florida State University, Tallahassee, FL 32306-4052, USA
[13,14]

A. Antonelli, G. Bencivenni, G. Bologna,[4] F. Bossi, P. Campana, G. Capon, D. Casper, V. Chiarella, G. Felici, P. Laurelli, G. Mannocchi,[5] F. Murtas, G.P. Murtas, L. Passalacqua, M. Pepe-Altarelli

Laboratori Nazionali dell'INFN (LNF-INFN), 00044 Frascati, Italy

L. Curtis, S.J. Dorris, A.W. Halley, I.G. Knowles, J.G. Lynch, V. O'Shea, C. Raine, J.M. Scarr, K. Smith, P. Teixeira-Dias, A.S. Thompson, E. Thomson, F. Thomson, R.M. Turnbull

Department of Physics and Astronomy, University of Glasgow, Glasgow G12 8QQ,United Kingdom[10]

O. Buchmüller, S. Dhamotharan, C. Geweniger, G. Graefe, P. Hanke, G. Hansper, V. Hepp, E.E. Kluge, A. Putzer, J. Sommer, K. Tittel, S. Werner, M. Wunsch

Institut für Hochenergiephysik, Universität Heidelberg, 69120 Heidelberg, Fed. Rep. of Germany[16]

R. Beuselinck, D.M. Binnie, W. Cameron, P.J. Dornan, M. Girone, S. Goodsir, E.B. Martin, A. Moutoussi, J. Nash, J.K. Sedgbeer, P. Spagnolo, A.M. Stacey, M.D. Williams

Department of Physics, Imperial College, London SW7 2BZ, United Kingdom[10]

V.M. Ghete, P. Girtler, D. Kuhn, G. Rudolph

Institut für Experimentalphysik, Universität Innsbruck, 6020 Innsbruck, Austria[18]

A.P. Betteridge, C.K. Bowdery, P.G. Buck, P. Colrain, G. Crawford, A.J. Finch, F. Foster, G. Hughes, R.W.L. Jones, T. Sloan, M.I. Williams

Department of Physics, University of Lancaster, Lancaster LA1 4YB, United Kingdom[10]

I. Giehl, A.M. Greene, C. Hoffmann, K. Jakobs, K. Kleinknecht, G. Quast, B. Renk, E. Rohne, H.-G. Sander, P. van Gemmeren, C. Zeitnitz

Institut für Physik, Universität Mainz, 55099 Mainz, Fed. Rep. of Germany[16]

J.J. Aubert, C. Benchouk, A. Bonissent, G. Bujosa, J. Carr, P. Coyle, C. Diaconu, F. Etienne, N. Konstantinidis, O. Leroy, F. Motsch, P. Payre, M. Talby, A. Sadouki, M. Thulasidas, K. Trabelsi

Centre de Physique des Particules, Faculté des Sciences de Luminy, IN^2P^3-CNRS, 13288 Marseille, France

M. Aleppo, M. Antonelli, F. Ragusa[2]

Dipartimento di Fisica, Università di Milano e INFN Sezione di Milano, 20133 Milano, Italy

R. Berlich, W. Blum, V. Büscher, H. Dietl, G. Ganis, C. Gotzhein, H. Kroha, G. Lütjens, G. Lutz, W. Männer, H.-G. Moser, R. Richter, A. Rosado-Schlosser, S. Schael, R. Settles, H. Seywerd, R. St. Denis, H. Stenzel, W. Wiedenmann, G. Wolf

Max-Planck-Institut für Physik, Werner-Heisenberg-Institut, 80805 München, Fed. Rep. of Germany[16]

J. Boucrot, O. Callot,[2] S. Chen, Y. Choi,[21] A. Cordier, M. Davier, L. Duflot, J.-F. Grivaz, Ph. Heusse, A. Höcker, A. Jacholkowska, M. Jacquet, D.W. Kim,[12] F. Le Diberder, J. Lefrançois, A.-M. Lutz, I. Nikolic, M.-H. Schune, S. Simion, E. Tournefier, J.-J. Veillet, I. Videau, D. Zerwas

Laboratoire de l'Accélérateur Linéaire, Université de Paris-Sud, IN^2P^3-CNRS, 91405 Orsay Cedex, France

P. Azzurri, G. Bagliesi,[2] G. Batignani, S. Bettarini, C. Bozzi, G. Calderini, M. Carpinelli, M.A. Ciocci, V. Ciulli, R. Dell'Orso, R. Fantechi, I. Ferrante, L. Foà,[1] F. Forti, A. Giassi, M.A. Giorgi, A. Gregorio, F. Ligabue, A. Lusiani, P.S. Marrocchesi, A. Messineo, F. Palla, G. Sanguinetti, A. Sciabà, J. Steinberger, R. Tenchini, G. Tonelli,[19] C. Vannini, A. Venturi, P.G. Verdini

Dipartimento di Fisica dell'Università, INFN Sezione di Pisa, e Scuola Normale Superiore, 56010 Pisa, Italy

G.A. Blair, L.M. Bryant, J.T. Chambers, Y. Gao, M.G. Green, T. Medcalf, P. Perrodo, J.A. Strong, J.H. von Wimmersperg-Toeller

Department of Physics, Royal Holloway & Bedford New College, University of London, Surrey TW20 OEX, United Kingdom[10]

D.R. Botterill, R.W. Clifft, T.R. Edgecock, S. Haywood, P.R. Norton, J.C. Thompson, A.E. Wright

Particle Physics Dept., Rutherford Appleton Laboratory, Chilton, Didcot, Oxon OX11 OQX, United Kingdom[10]

B. Bloch-Devaux, P. Colas, S. Emery, W. Kozanecki, E. Lançon, M.C. Lemaire, E. Locci, P. Perez, J. Rander, J.-F. Renardy, A. Roussarie, J.-P. Schuller, J. Schwindling, A. Trabelsi, B. Vallage

CEA, DAPNIA/Service de Physique des Particules, CE-Saclay, 91191 Gif-sur-Yvette Cedex, France[17]

S.N. Black, J.H. Dann, R.P. Johnson, H.Y. Kim, A.M. Litke, M.A. McNeil, G. Taylor

Institute for Particle Physics, University of California at Santa Cruz, Santa Cruz, CA 95064, USA[22]

C.N. Booth, R. Boswell, C.A.J. Brew, S. Cartwright, F. Combley, M.S. Kelly, M. Lehto, W.M. Newton, J. Reeve, L.F. Thompson

Department of Physics, University of Sheffield, Sheffield S3 7RH, United Kingdom[10]

A. Böhrer, S. Brandt, G. Cowan, C. Grupen, G. Lutters, P. Saraiva, L. Smolik, F. Stephan

Fachbereich Physik, Universität Siegen, 57068 Siegen, Fed. Rep. of Germany[16]

M. Apollonio, L. Bosisio, R. Della Marina, G. Giannini, B. Gobbo, G. Musolino

Dipartimento di Fisica, Università di Trieste e INFN Sezione di Trieste, 34127 Trieste, Italy

J. Rothberg, S. Wasserbaech

Experimental Elementary Particle Physics, University of Washington, WA 98195 Seattle, U.S.A.

S.R. Armstrong, E. Charles, P. Elmer, D.P.S. Ferguson, S. González, T.C. Greening, O.J. Hayes, H. Hu, S. Jin, P.A. McNamara III, J.M. Nachtman, J. Nielsen, W. Orejudos, Y.B. Pan, Y. Saadi, I.J. Scott, J. Walsh, Sau Lan Wu, X. Wu, J.M. Yamartino, G. Zobernig

Department of Physics, University of Wisconsin, Madison, WI 53706, USA[11]

[1] Now at CERN, 1211 Geneva 23, Switzerland.
[2] Also at CERN, 1211 Geneva 23, Switzerland.
[3] Also at Dipartimento di Fisica, INFN, Sezione di Catania, Catania, Italy.
[4] Also Istituto di Fisica Generale, Università di Torino, Torino, Italy.
[5] Also Istituto di Cosmo-Geofisica del C.N.R., Torino, Italy.
[6] Supported by the Commission of the European Communities, contract ERBCHBICT941234.
[7] Supported by CICYT, Spain.
[8] Supported by the National Science Foundation of China.
[9] Supported by the Danish Natural Science Research Council.
[10] Supported by the UK Particle Physics and Astronomy Research Council.
[11] Supported by the US Department of Energy, grant DE-FG0295-ER40896.
[12] Permanent address: Kangnung National University, Kangnung, Korea.
[13] Supported by the US Department of Energy, contract DE-FG05-92ER40742.
[14] Supported by the US Department of Energy, contract DE-FC05-85ER250000.
[15] Permanent address: Universitat de Barcelona, 08208 Barcelona, Spain.
[16] Supported by the Bundesministerium für Bildung, Wissenschaft, Forschung und Technologie, Fed. Rep. of Germany.
[17] Supported by the Direction des Sciences de la Matière, C.E.A.
[18] Supported by Fonds zur Förderung der wissenschaftlichen Forschung, Austria.
[19] Also at Istituto di Matematica e Fisica, Università di Sassari, Sassari, Italy.
[20] Now at Princeton University, Princeton, NJ 08544, U.S.A.
[21] Permanent address: Sung Kyun Kwan University, Suwon, Korea.
[22] Supported by the US Department of Energy, grant DE-FG03-92ER40689.
[23] Now at School of Operations Research and Industrial Engineering, Cornell University, Ithaca, NY 14853-3801, U.S.A.
[24] Now at Schweizerischer Bankverein, Basel, Switzerland.

1 Introduction

Measurements of individual b hadron lifetimes are of interest as they test theoretical understanding of b hadron decay dynamics. No case has been more intriguing than that of the b baryon. Previous measurements of $\tau(\Lambda_b)$ have shown it to be significantly shorter than the B meson lifetime [1], in contrast to theoretical predictions [2, 3]. In the simple spectator model, the lifetimes of the b hadrons are equal. When interactions involving the spectator quark are included, theory predicts small lifetime differences between species. Indeed, understanding the short Λ_b lifetime has been named one of the problems in heavy quark theory.

Evidence for b baryons in Z decays was first established via $\Lambda\ell^-$ combinations[1] in $Z \to b\overline{b}$ decay [4] and subsequently with $\Lambda_c^+\ell^-$ pairs [5]. Both samples have been used previously by ALEPH to measure the lifetime – in the first, the average over all b baryons decaying to Λ, and in the second, that of the Λ_b exclusively [6]. This paper presents the lifetime of b baryons measured with three independent methods: refined versions of the two previously published plus a third analysis based on partially reconstructed Λ_c^+'s. The first method, based upon the lepton impact parameter distribution of high transverse momentum leptons from $\Lambda_b \to \Lambda\ell^-\overline{\nu}X$ decays, gives the highest statistical precision. The second relies on full reconstruction of Λ_c^+'s paired with high momentum leptons, corresponding to the decay $\Lambda_b \to \Lambda_c^+\ell^-\overline{\nu}X$. The third employs a similar technique, but uses partially reconstructed Λ_c^+ candidates, namely $\Lambda_b \to \Lambda_c^+\ell^-\overline{\nu}X$ with $\Lambda_c^+ \to \Lambda\ell^+X$. In addition, the product branching fractions to each observed final state are measured, essential inputs in determining the various b hadron fractions in hadronic Z decay [7].

The current measurements use a sample of about 4 million hadronic Z decays, recorded from 1991 to 1995. In addition to the increased data sample, these current measurements improve on the previous ALEPH results [6] via the reconstruction of new decay modes and better selection efficiency, yielding twice the number of observed $\Lambda\ell^-$ combinations with an increased sample purity and about four times as many $\Lambda_c^+\ell^-$ events reconstructed. The third analysis is new and provides an additional source of reconstructed events. These measurements supersede the previous results.

The following sections describe the ALEPH detector, the measurement of the b baryon lifetime and branching fractions extracted from analysis of the lepton impact parameter spectrum of the $\Lambda\ell^-$ sample, the measurement of $\tau(\Lambda_b)$ from the proper time distribution of exclusively reconstructed Λ_c^+'s paired with leptons, $\tau(\Lambda_b)$ measured from the proper times of partially reconstructed Λ_c^+'s correlated with a second lepton, and the branching fractions of Λ_b measured from partially and fully reconstructed Λ_c^+'s.

2 The ALEPH detector

The ALEPH detector and its performance are described in detail elsewhere [8, 9, 10], only a brief overview will be given here. The subdetectors critical to this measurement are the tracking chambers for precise impact parameter and decay length reconstruction, and the electromagnetic and hadronic calorimeters and the muon chambers, for missing energy measurement and for lepton identification.

A high resolution vertex detector (VDET) consisting of two layers of double-sided silicon

[1] In this paper lepton, ℓ, refers to either an electron or a muon. In addition, charge conjugate reactions are always implied.

microstrip detectors surrounds the beam pipe. The inner layer is 6.5 cm from the beam axis and covers 85% of the solid angle and the outer layer is at an average radius of 11.3 cm and covers 69%. The spatial resolution for the $r\phi$ and z projections (transverse to and along the beam axis, respectively) is 12 μm at normal incidence. The vertex detector is surrounded by a drift chamber (ITC) with eight coaxial wire layers with an outer radius of 26 cm and by a time projection chamber (TPC) that measures up to 21 three-dimensional points per track at radii between 30 cm and 180 cm. These detectors are immersed in an axial magnetic field of 1.5 T and together measure the transverse momentum $p_{\rm T}$, relative to the beam axis, of charged particles with a resolution $\sigma(p_{\rm T})/p_{\rm T} = 6 \times 10^{-4} p_{\rm T} \oplus 0.005$ ($p_{\rm T}$ in GeV/c). The resolution of the three-dimensional impact parameter in the transverse and longitudinal views for tracks having information from all tracking detectors and two VDET hits can be parameterized as $\sigma = 25\mu{\rm m} + 95\mu{\rm m}/p$ (p in GeV/c). The TPC also provides up to 338 measurements of the specific ionization of a charged track ($\mathrm{d}E/\mathrm{d}x$). For electrons in hadronic events, the $\mathrm{d}E/\mathrm{d}x$ resolution is 4.5% for 338 ionization samples. The TPC is surrounded by an electromagnetic calorimeter of lead/proportional–chamber construction segmented into $0.9^\circ \times 0.9^\circ$ projective towers read out in three sections in depth, with energy resolution $\sigma(E)/E = 0.18/\sqrt{E} + 0.009$ (E in GeV). The iron return yoke of the magnet is instrumented with streamer tubes to form a hadron calorimeter with a thickness of over 7 interaction lengths and is surrounded by two additional double-layers of streamer tubes to aid in muon identification. An algorithm combines all these measurements to provide a determination of the energy flow [10] with a precision on the measurable total visible energy of $\sigma(E) = 0.6\sqrt{E/\mathrm{GeV}} + 0.6$ GeV. Electrons are identified using the electromagnetic calorimeter together with the $\mathrm{d}E/\mathrm{d}x$ information from the TPC [10]. Muons are identified by their characteristic penetration pattern in the hadron calorimeter together with the muon chambers [10].

The selection of hadronic events is based on charged tracks and is described in Ref. [11]. The interaction point is reconstructed on an event-by-event basis using the constraint of the average beam spot position [10]. The resolution is 85 μm for $\mathrm{Z} \to \mathrm{b\overline{b}}$ events, projected along the sphericity axis of the event.

3 Measurement of lifetime and branching fractions of b baryons using $\Lambda\ell^-$ combinations

Semileptonic b baryon decays are selected using the correlation between a Λ and a lepton reconstructed in the same hemisphere, defined by the plane perpendicular to the thrust axis. This method is sensitive to decays of all species of b baryon which have $\Lambda\ell^-$ in the final state, mainly $\Lambda_{\rm b}$ but also $\Xi_{\rm b}$ or $\Omega_{\rm b}$. For brevity of notation, the symbols $\Lambda_{\rm b}$ and $\Lambda_{\rm c}^+$ are used throughout this section to denote generic b and c baryons.

The Λ candidates are reconstructed in the channel $\Lambda \to \mathrm{p}\pi^-$, with an algorithm which fits two oppositely charged particle tracks to a common vertex [10]. The candidate leptons are identified using the method described in Ref. [10]. The requirements applied to the Λ candidates are similar to those in Ref. [6]. To further reduce background, the cut on the momentum of the Λ candidate has been increased from 3 GeV/c to 4 GeV/c. To improve the resolution in the impact parameter measurement, the lepton candidates are required, as in Ref. [6], to have at least one associated $r\phi$ coordinate in the VDET, 5 hits in the TPC and 2 hits in the ITC and a

χ^2/d.o.f. for the track fit of less than 4. Lepton and Λ candidates are required to be within 45 degrees of each other.

The possible sources of $\Lambda\ell$ combinations with their estimated contributions to the right-sign $\Lambda\ell^-$ and wrong-sign $\Lambda\ell^+$ samples after all the selection criteria are applied are listed in Table 1.

Source	Estimated $\Lambda\ell^-$	Estimated $\Lambda\ell^+$
1) $\Lambda_b \to \Lambda_c^+ X\ell^-\overline{\nu}$, $\Lambda_c^+ \to \Lambda X$	705 ± 69	-
2) $\Lambda_b \to \Lambda_c^+ X\tau^-\overline{\nu}$, $\Lambda_c^+ \to \Lambda X$, $\tau^- \to \ell^-\nu\overline{\nu}$	13 ± 4	-
3) $\Lambda_b \to \Lambda_c^+ D_s^- X$, $\Lambda_c^+ \to \Lambda X$, $D_s^- \to X\ell^-\overline{\nu}$	9 ± 9	-
4) $\Lambda_b \to J/\psi \Lambda X$, $J/\psi \to \ell^+\ell^-$	6 ± 3	6 ± 3
5) $\overline{B} \to \Lambda_c^+ X\ell^-\overline{\nu}$, $\Lambda_c^+ \to \Lambda X$	4 ± 4	4 ± 4
6) $b \to \Lambda_c^+ X$, $\Lambda_c^+ \to \Lambda\ell^+ X$	-	45 ± 14
7) $\Lambda_c^+ \to \Lambda\ell^+ X$	-	13 ± 4
8) Λ from fragmentation	184 ± 60	230 ± 40
9) Fake $\Lambda\ell$ combinations	142 ± 28	142 ± 28
Total number of $\Lambda\ell$ combinations	1063	441

Table 1: Sources of $\Lambda\ell$ combinations estimated from the total number of $\Lambda\ell^-$ and $\Lambda\ell^+$ candidates selected in the data, as described in the text.

Process (1) is the signal of semileptonic b baryon decays. Processes (2), (3) and (4) are considered in the lifetime fit as an additional contribution of b baryons to the $\Lambda\ell^-$ sample. The requirement of a lepton candidate with a momentum of at least 3 GeV/c and a transverse momentum $p_\perp$ with respect to the associated jet[2] of at least 1 GeV/c removes most of the $\Lambda\ell$ combinations from processes (2) to (7). The remaining background is mainly due to fragmentation Λ's (8) and fake combinations (9). The former are accidental combinations of a prompt Λ produced in the quark fragmentation associated with a candidate lepton in the same hemisphere. Fake combinations are spurious $p\pi^-$ combinations under the Λ invariant mass peak paired with a candidate lepton or fake leptons paired with a non-fragmentation Λ. The fragmentation Λ background is reduced by the 4 GeV/c cut on the momentum of the candidate Λ. Fake $p\pi^-$ combinations are reduced by requiring the Λ decay vertex to be at least 5 cm from the interaction point and, when available, the dE/dx measurements for the candidate proton and pion to be within three standard deviations of the expectations.

The $p\pi$ invariant mass spectra of the reconstructed $\Lambda\ell^-$ and $\Lambda\ell^+$ combinations are shown in Fig. 1. Candidate Λ's are selected by means of a Λ momentum dependent mass window

[2]The lepton is included in the calculation of the jet direction.

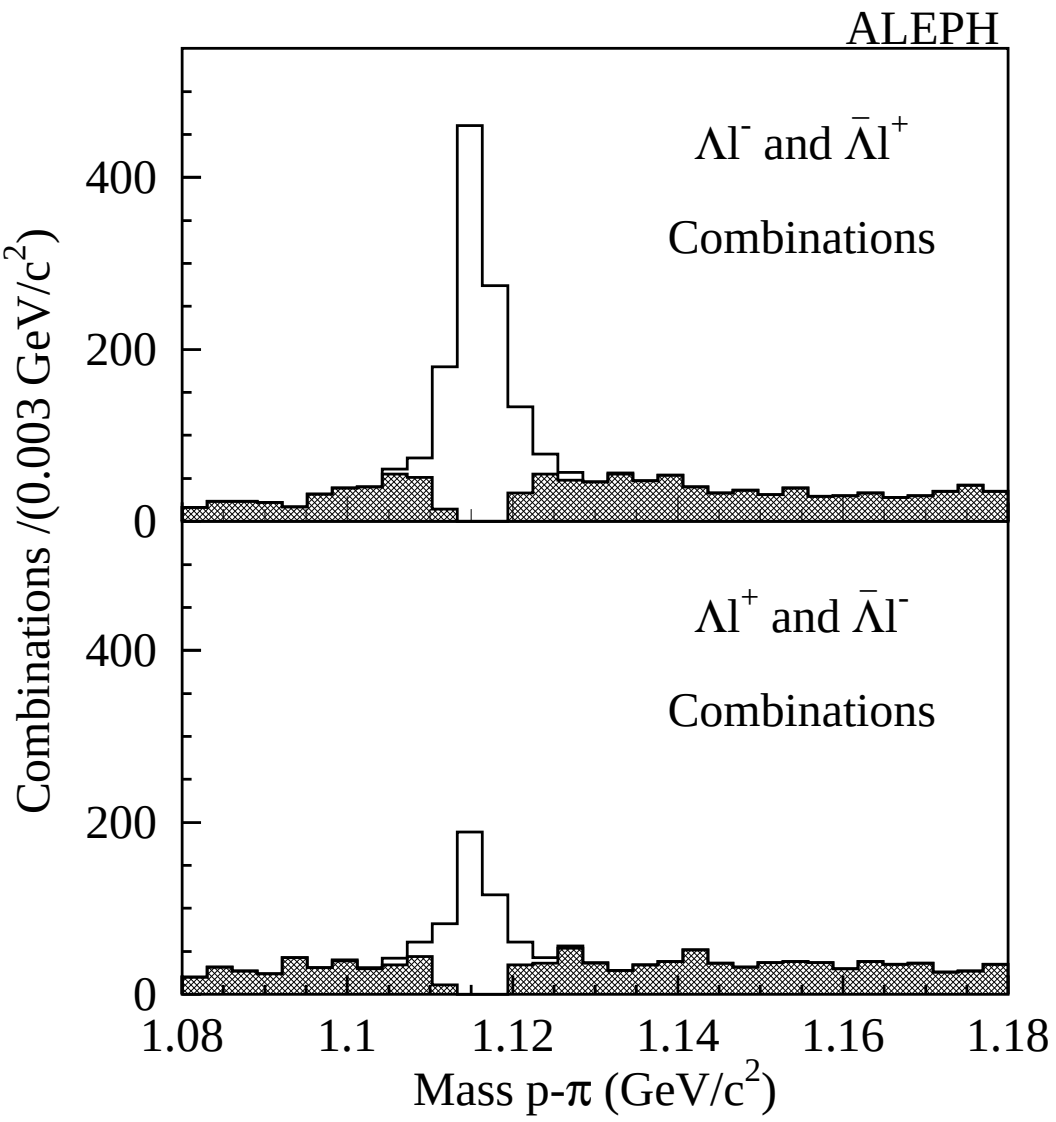

Figure 1: The pπ invariant mass distribution for the right-sign $\Lambda\ell^-$ and wrong-sign $\Lambda\ell^+$ combinations observed in the data. The unshaded areas correspond to the selected events within the momentum dependent mass window cut.

cut of $\pm 2\sigma(p_\Lambda)$ around the nominal Λ mass, since the Λ mass resolution depends on the Λ momentum [12]. The average value of σ is about 3 MeV/c^2. The total selection yields 1063 right-sign $\Lambda\ell^-$ candidates and 441 wrong-sign $\Lambda\ell^+$ candidates.

The right-sign excess is mainly due to semileptonic b baryon decays. In order to estimate the number of b baryon events in the $\Lambda\ell^-$ sample, the contribution of the right and wrong-sign background is evaluated. The contribution of the physical processes (2)-(7), relative to semileptonic b baryon decay (1), is estimated from a study based on 5 million Monte Carlo $Z\to q\overline{q}$ events simulated with JETSET 7.4 [13] tuned to ALEPH data, as described in Ref [14]. The contribution of fragmentation Λ's (8) in the right-sign is estimated from the number of wrong-sign $\Lambda\ell^+$ events observed in the data, after subtraction of the combinatorial background (9) and the semileptonic Λ_c^+ decays (6),(7). In addition a correction is applied for the imbalance of the fragmentation Λ background between right and wrong-sign combinations. This imbalance is mainly caused by an enhancement of the combinations of fragmentation Λ's associated with $\bar{\Lambda}_b \to \ell^+$ in the $\Lambda\ell^+$ sample and a suppression of combinations with $\Lambda_b \to \ell^-$ in the $\Lambda\ell^-$ sample. The ratio of the $\Lambda\ell^-$ to $\Lambda\ell^+$ fragmentation Λ background is estimated, using simulated $Z\to q\overline{q}$ events, to be 0.80 ± 0.20, where the error reflects mainly the uncertainty in the production of Λ baryons in the process of b fragmentation. The fraction of the combinatorial background (9) to the $\Lambda\ell^-$ sample is estimated from simulation, in agreement with the estimate from a fit to the $p\pi^-$ invariant distribution observed in the data.

The estimated contributions of the various processes to the $\Lambda\ell$ combinations are reported in Table 1. The resulting fraction of semileptonic b baryon decays in the selected $\Lambda\ell^-$ sample is $66 \pm 6\%$, which corresponds to $705 \pm 32(\text{stat}) \pm 62(\text{syst})$ events.

3.1 b baryon lifetime fit

The b baryon lifetime is determined by a maximum likelihood fit to the $r\phi$ impact parameter distribution of the lepton candidates in the $\Lambda\ell^-$ sample. The fitting procedure is the same as was used in the previous ALEPH measurement of the b baryon lifetime [6]. The total lepton impact parameter distribution for the $\Lambda\ell^-$ sample is a sum of various components describing each lepton source. Table 2 shows their relative contributions to the $\Lambda\ell^-$ sample.

The impact parameter distribution for prompt lepton sources (the first five components in Table 2) is obtained by convoluting a resolution function with the physics function which describes the expected impact parameter distribution in the case of perfect detector resolution. The physics function is obtained separately for each prompt lepton source from a Monte Carlo simulation of the decay process. The scale of the physics function is set by the corresponding lifetime. The $\Lambda_b \to \ell$ and $\Lambda_b \to c/\tau \to \ell$ physics functions depend on the b baryon lifetime, the only parameter of the fit, while the background physics functions, $b \to \ell$ and $b \to c/\tau \to \ell$ depend on the average b hadron lifetime and the $c \to \ell$ function depends on the c hadron lifetimes. The fragmentation Λ and combinatorial background $\Lambda\ell^-$ combinations are described with different shapes of physics functions and different b lifetimes. The difference in the shape of the physics functions is due to a difference in the momentum spectrum of the candidate Λ's and leptons for the two processes. Different lifetimes are used because the b hadron composition is different for the two backgrounds. In order to reduce the systematic uncertainty due to the simulation, the b lifetime for the fake $\Lambda\ell^-$ combinations is obtained from the data by fitting the right-sign sideband of the $p\pi$ invariant mass while the b lifetime for the accidental $\Lambda\ell^-$ is assumed to be the measured average b hadron lifetime. The sideband is defined as the region

Lepton source	$\Lambda\ell^-$ source in Table 1	fraction in %
$\Lambda_b \to \ell$	(1)	66.3 ± 5.9
$\Lambda_b \to (c/\tau) \to \ell$	(2),(3),(4)	2.7 ± 1.2
$b \to \ell$	(5),(8),(9)	23.3 ± 4.7
$b \to (c/\tau) \to \ell$	(8),(9)	3.0 ± 0.9
$c \to \ell$	(8),(9)	1.5 ± 0.5
Misidentified hadrons	(8),(9)	1.4 ± 0.7
π, K decays and γ conversions	(8),(9)	1.8 ± 0.9

Table 2: Lepton sources in the $\Lambda\ell^-$ sample with the corresponding $\Lambda\ell^-$ sources according to Table 1. The fraction of signal $\Lambda_b \to \ell$ is obtained using the data, as described previously, while the other lepton sources are estimated from the Monte Carlo.

of the $p\pi$ invariant mass outside the Λ peak, hence when the $p\pi$ invariant mass, $M_{p\pi} > 1.146$ GeV/c^2 and $M_{p\pi} < 1.250$ GeV/c^2.

The resolution function describes the detector effects on the measurement of the impact parameter of the candidate leptons. It is derived from simulated events and is parametrised with a double Gaussian function. Corrections to the width and amplitude of the Gaussian functions at the level of 10% are applied to account for the difference in the impact parameter resolution of hadron tracks observed between data and Monte Carlo events, as described in Ref. [6] and [15].

The expected impact parameter distribution for hadrons misidentified as leptons is obtained from the impact parameter distribution of hadrons selected in the data with the same requirements as applied to the leptons candidates except the lepton identification. The impact parameter distribution of leptons coming from K and π decays in flight is taken from simulation.

The unbinned maximum likelihood fit to the lepton impact parameter distribution of the 1063 $\Lambda\ell^-$ candidates yields a b baryon lifetime of

$$\tau(\text{b baryon}) \;=\; 1.20 \pm 0.08 \text{ ps},$$

where the quoted error is statistical. Fig. 2 shows the result of the fit and the observed impact parameter distribution of the lepton candidates in the $\Lambda\ell^-$ sample. The fit to the 2207 $p\pi$ sideband events yields a background lifetime for the fake $\Lambda\ell^-$ combinations of $\tau_{b-comb} = 1.50 \pm 0.05$ ps.

3.2 Systematic errors

The various contributions to the systematic uncertainty in the b baryon lifetime measurement are listed in Table 3.

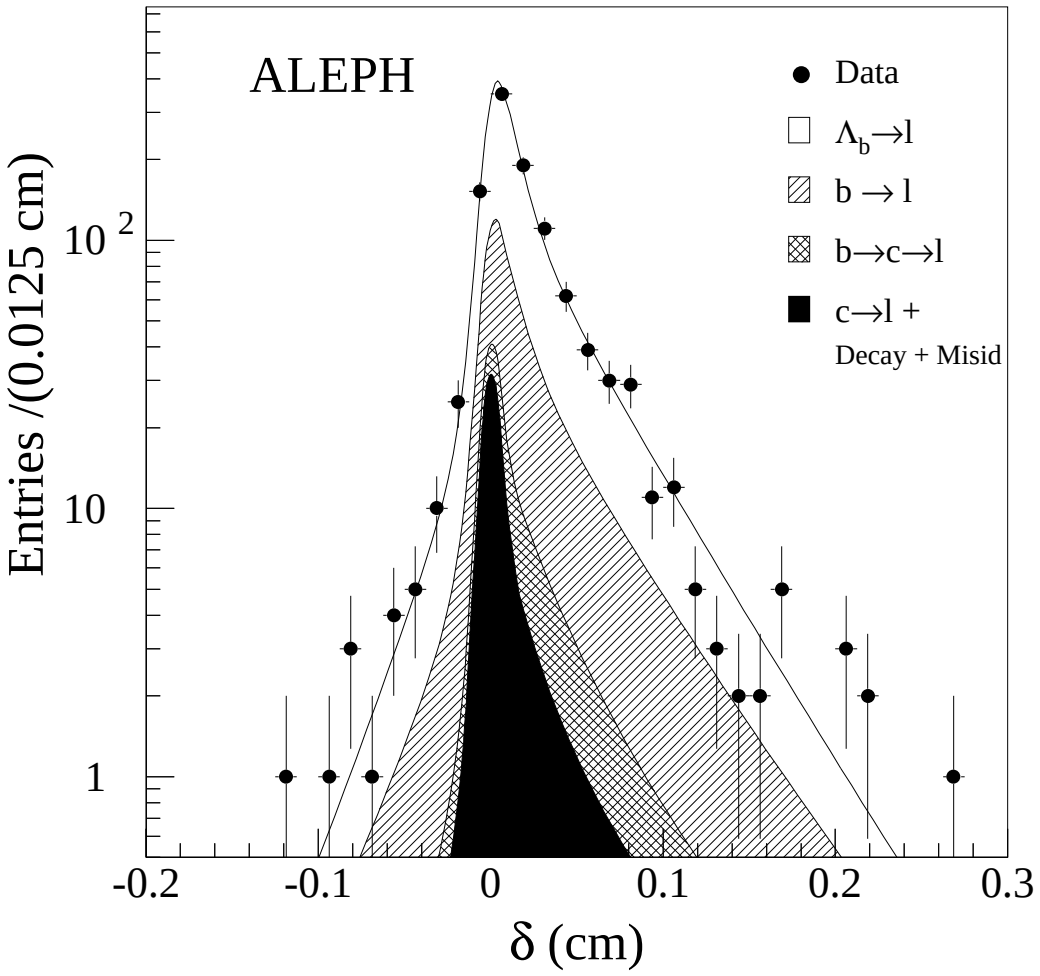

Figure 2: Lepton impact parameter (δ) distribution of the selected $\Lambda\ell^-$ candidates. The solid curve is the probability function at the fitted value of the lifetime, while the shaded areas show, one on top of the other, the background contributions.

One of the major contributions to the systematic error arises from the lack of knowledge of the Λ_b polarisation. The $\Lambda_b \to \ell$ physics function is sensitive to the polarisation of the Λ_b because the impact parameter of the lepton is correlated with its decay angle. The shape of the $\Lambda_b \to \ell$ physics function is determined using the JETSET 7.4 [13] Monte Carlo simulation corrected by assigning weights to each event according to the measured ALEPH value of the Λ_b polarisation of $\mathcal{P}_{\Lambda_b} = -23^{+25}_{-21}$ % [16].

A further systematic uncertainty is due to the uncertainties in the parameters of the physics function which are used for the signal $\Lambda_b \to \ell$ and $\Lambda_b \to c/\tau \to \ell$ and for the backgrounds $b \to \ell$, $b \to c/\tau \to \ell$ and $c \to \ell$. The parameters of each physics function are varied within their uncertainties, estimated by fitting the expected impact parameter distribution in simulated events.

The systematic uncertainty due to the impact parameter resolution is estimated from the variation of the fitted lifetime when the corrections to the resolution function parametrisation are removed. The full difference of the fitted lifetime is taken as a systematic uncertainty, symmetric around the central value.

The uncertainty in the number of combinatorial background events in the right-sign sample (see Table 1) is estimated to be 20% by comparing the $p\pi$ invariant mass distribution in data and Monte Carlo. The uncertainty due to the contribution of the background of fragmentation Λ's is estimated by varying the production imbalance between right-sign and wrong-sign fragmentation Λ's by ± 0.20.

The fractions of the lepton sources for the background, shown in Table 2, are obtained from the Monte Carlo simulation and their uncertainties translated into a systematic error on the b baryon lifetime.

The effective lifetime of the $b \to \ell$ physics functions for the fragmentation Λ background is taken to be the inclusive b hadron lifetime [1]. In addition to the uncertainty in the inclusive b hadron lifetime, a variation of $+0.04$ ps in the lifetime is considered. This covers the possibility of a complete suppression of b baryons in the fragmentation $\Lambda\ell^-$combinations. The uncertainty in the effective lifetime of the combinatorial background is estimated from the statistical error on the lifetime fit to the $p\pi^-$ sideband.

The determination of the physics functions depends on the modeling of semileptonic b baryon decay and on b fragmentation. The physics functions are estimated from a Monte Carlo simulation of $\Lambda_b \to \ell$ with a four-body semileptonic b baryon decay of $20 \pm 20\%$ (relative to the total semileptonic decay rate), which leads to a systematic uncertainty in the b baryon lifetime. The systematic uncertainty due to the b baryon fragmentation is estimated from a variation of the Peterson function [17] which covers an uncertainty in the average b baryon momentum ($\langle x_{\mathrm{b-baryon}} \rangle = 0.715 \pm 0.030$) double that measured from a sample of B mesons [18].

A systematic uncertainty due to the simulation of the impact parameter distribution for the π and K decays in flight is estimated by varying the parametrisation of the function used in the lifetime fit. The uncertainty due to the parametrisation of the impact parameter distributions for hadrons misidentified as candidate leptons is negligible, since the distribution is obtained directly using the data.

The uncertainty in the number of $\Lambda\ell$ combinations arising from physics decay processes (sources (2) to (7) in Table 1) affects the estimation of the b baryon sample purity and leads to a small systematic uncertainty in the measured lifetime.

Summing all the contributions in quadrature, the total systematic error on the b baryon lifetime is estimated to be ± 0.06 ps. In conclusion, the b baryon lifetime measured using $\Lambda\ell^-$

Source of systematic error	Uncertainty (ps)
Λ_b polarisation ($\mathcal{P}_{\Lambda_b} = -23^{+25}_{-21}\%$)	$^{-0.037}_{+0.031}$
Signal physics functions	± 0.032
Background physics functions	± 0.016
Resolution function	± 0.021
Background lepton source fractions	± 0.015
Number of combinatorial $\Lambda\ell^-$ ($\pm 20\%$)	∓ 0.017
Ratio of accidental $\Lambda\ell^-$/ $\Lambda\ell^+$ (R$= 0.80 \pm 0.20$)	∓ 0.010
τ fragmentation backg. ($\tau_{b-frag} = 1.55^{+0.04}_{-0.02}$ ps)	$^{-0.010}_{+0.005}$
τ combinatorial backg. ($\tau_{b-comb} = 1.50 \pm 0.05$ ps)	∓ 0.010
Λ_b decay model (4-body decay $20 \pm 20\%$)	± 0.015
b baryon fragmentation ($\langle x_{\Lambda_b} \rangle = 0.715 \pm 0.030$)	∓ 0.014
Decay background and Misid function	± 0.007
Additional $\Lambda\ell$ physics sources	± 0.005
Total	$^{+0.063}_{-0.066}$

Table 3: Contributions to the systematic uncertainty in the b baryon lifetime measurement. The sign of each uncertainty is correlated with the corresponding variation, where reported.

combinations is

$$\tau(\text{b baryon}) \;=\; 1.20 \pm 0.08(\text{stat}) \pm 0.06(\text{syst}) \text{ ps} \,.$$

This result supersedes the previous ALEPH measurement [6].

3.3 Measurement of the b baryon production rate

For the the product branching ratio measurement, the requirements for the candidate lepton track to have at least one associated $r\phi$ coordinate in the VDET and two hits in the ITC are removed. These requirements are necessary for ensuring a reliable impact parameter measurement but in the case of the branching ratio measurement they reduce the sample statistics and they introduce an additional uncertainty due to the simulation of the related efficiency. This selection yields 1319 $\Lambda\ell^-$ combinations from 4,029,548 hadronic events and $866 \pm 36(\text{stat}) \pm 78(\text{syst})$ $\Lambda\ell^-$ candidates are attributed to b baryon semileptonic decays. The reconstruction efficiency for the signal process $\Lambda_\text{b} \to \Lambda\ell^-$ is $7.5 \pm 0.1(\text{stat}) \pm 0.6(\text{syst})\%$. The efficiency contains the measured branching ratio of $\Lambda \to \text{p}\pi^-$ [1]. Using the ALEPH measurement of R_b [19], the product branching ratio, averaged over electron and muon channels, is

$$\text{Br}(\text{b} \to \Lambda_\text{b}) \cdot \text{Br}(\Lambda_\text{b} \to \Lambda_\text{c}^+ \ell^- \overline{\nu} \text{X}) \cdot \text{Br}(\Lambda_\text{c}^+ \to \Lambda \text{X}) = (0.326 \pm 0.016(\text{stat}) \pm 0.039(\text{syst}))\,\% \,.$$

The systematic uncertainty is dominated by the uncertainty in the estimation of the efficiency and in the subtraction of the $\Lambda\ell^-$ background combinations. The uncertainties in the efficiency are mainly due to a difference in the mass resolution between data and Monte Carlo and to the simulation of the b baryon production (b quark fragmentation) and decay (semileptonic decay model). This result supersedes the previous ALEPH measurement [6].

4 Measurement of the Λ_b lifetime using $\Lambda_\text{c}^+\ell^-$ combinations

A complementary measurement of the Λ_b lifetime is based on the selection of the semileptonic decays $\Lambda_\text{b} \to \Lambda_\text{c}^+ \ell^- \bar{\nu}$ with exclusive reconstruction of the Λ_c^+. Whereas the first method ($\Lambda\ell^-$) averages over all b baryons, this sample is expected to have a large contribution from semileptonic Λ_b decay. The $\Lambda_\text{c}^+\ell^-$ combinations allow a measurement of the Λ_b decay vertex and hence its decay length on an event-by-event basis. From the decay length and an estimate of the Λ_b momentum it is possible to estimate the proper time and extract the Λ_b lifetime by performing a maximum likelihood fit. The available $\Lambda_\text{c}^+\ell^-$ sample is about three times larger than the previous published result [6] due to the inclusion of the data collected during 1994 and 1995 and the reconstruction of the Λ_c^+ decay in one additional channel ($\Lambda\pi$). This method has fewer events but smaller systematic effects than the previous one.

4.1 Selection of Λ_b using $\Lambda_\text{c}^+\ell^-$ combinations

There are five main sources of $\Lambda_\text{c}^+\ell^-$ pairs: the signal process (1) in Table 1, the background processes (2), (3), and (5), and combinatorial background which is mainly fake Λ_c^+ associated with a real or fake lepton.

Candidates for the decay $\Lambda_b \to \Lambda_c^+ \ell^- \bar{\nu}$ are identified in hadronic Z events where a Λ_c^+ is associated with a lepton in the same hemisphere. The Λ_c^+ candidates are reconstructed in four decay modes, namely $\Lambda_c^+ \to pK^-\pi^+$, $\Lambda_c^+ \to p\bar{K}^0$, $\Lambda_c^+ \to \Lambda\pi^+\pi^+\pi^-$ and $\Lambda_c^+ \to \Lambda\pi^+$. The standard ALEPH lepton identification, described in [10], is used in this analysis. The selection procedure for the Λ_c^+ is similar to that used in [6].

In the $\Lambda_c^+ \to pK^-\pi^+$ channel, the proton, kaon and pion candidates are required to have momenta greater than 4, 2 and 1 GeV/c, respectively. The TPC dE/dx measurement for proton candidates is required to be available and within three standard deviations of that expected for protons. Inconsistency with the pion hypothesis is also demanded by requiring the dE/dx measurement to be at least 2 standard deviations away from that expected for pions of similar momenta. For kaon and pion candidates the specific ionization is required, when available, to be within 3 standard deviations of that expected. This channel suffers most from combinatorial background, which is suppressed by introducing a cut on $l_{\Lambda_c}/\sigma_{l_{\Lambda_c}} > -0.5$, where l_{Λ_c} is the distance between the Λ_b and the Λ_c^+ vertices projected onto the Λ_c^+ momentum. According to studies with simulated events, this cut introduces a negligible bias on the Λ_b lifetime. The $\Lambda_c^+ \to \Lambda\pi^+\pi^+\pi^-$ candidates are selected with a Λ having momentum greater than 3 GeV/c and three pions with momenta greater than 0.5 GeV/c. The Λ selection has been described already in Section 3. For the $\Lambda_c^+ \to \Lambda\pi^+$channel, the Λ is associated with a pion with momentum greater than 3.5 GeV/c and the dE/dx measurement, when available, is required to be consistent with the pion hypothesis. For the $\Lambda_c^+ \to p\bar{K}^0$ decay channel, the proton and the K_S^0 candidates are required to have momenta greater than 3.5 and 2 GeV/c, respectively. The K_S^0 candidates are identified by their decay $K_S^0 \to \pi^+\pi^-$, with the same algorithm used for the Λ selection. The cosine of the proton decay angle in the Λ_c^+ rest frame must be greater than -0.8 to reduce the combinatorial background.

In the four channels, Λ_c^+ candidates with momentum greater than 8 GeV/c are selected and combined with an identified lepton with momentum above 3 GeV/c in a 45° cone around the Λ_c^+ direction in the same event hemisphere. The $\Lambda_c^+\ell^-$ system is required to have a momentum greater than 20 GeV/c and an invariant mass above 3.5 GeV/c^2. These two requirements reduce the combinatorial background and the contribution of background from non b semileptonic decays. For the measurement of the Λ_b lifetime, further requirements on the track quality and vertex fits are applied. To ensure a good reconstruction of the decay length, the lepton and at least two of the charged tracks from the $\Lambda_c^+ \to pK^-\pi^+$ and $\Lambda_c^+ \to \Lambda\pi^+\pi^+\pi^-$ candidates are required to have one or more associated hits in the VDET. For the $\Lambda_c^+ \to p\bar{K}^0$ and $\Lambda_c^+ \to \Lambda\pi^+$ decays this requirement is applied to the lepton and the proton/pion candidates. The χ^2 probability of the Λ_c^+ and the Λ_b vertex fits are required to be greater than 1%.

These criteria yield a final sample of 193 $\Lambda_c^+\ell^-$ combinations selected in a $\pm 2\sigma$ window around the nominal Λ_c^+ mass. The mass resolution σ is estimated from the Monte Carlo. Fig. 3 shows the individual contributions of the four Λ_c^+ decay channels to the right and wrong-sign $\Lambda_c\ell$ combinations, while Fig. 4 shows their sum after all cuts. A clear signal is observed at the nominal Λ_c^+ mass in the right-sign $\Lambda_c^+\ell^-$ combinations while for wrong-sign $\Lambda_c^+\ell^+$ events no such enhancement is observed.

Table 4 summarises the number of $\Lambda_c^+\ell^-$ candidates selected in the four Λ_c^+ decay channels. The fraction of combinatorial background within the mass window is estimated from a straight line fit to the invariant mass distributions.

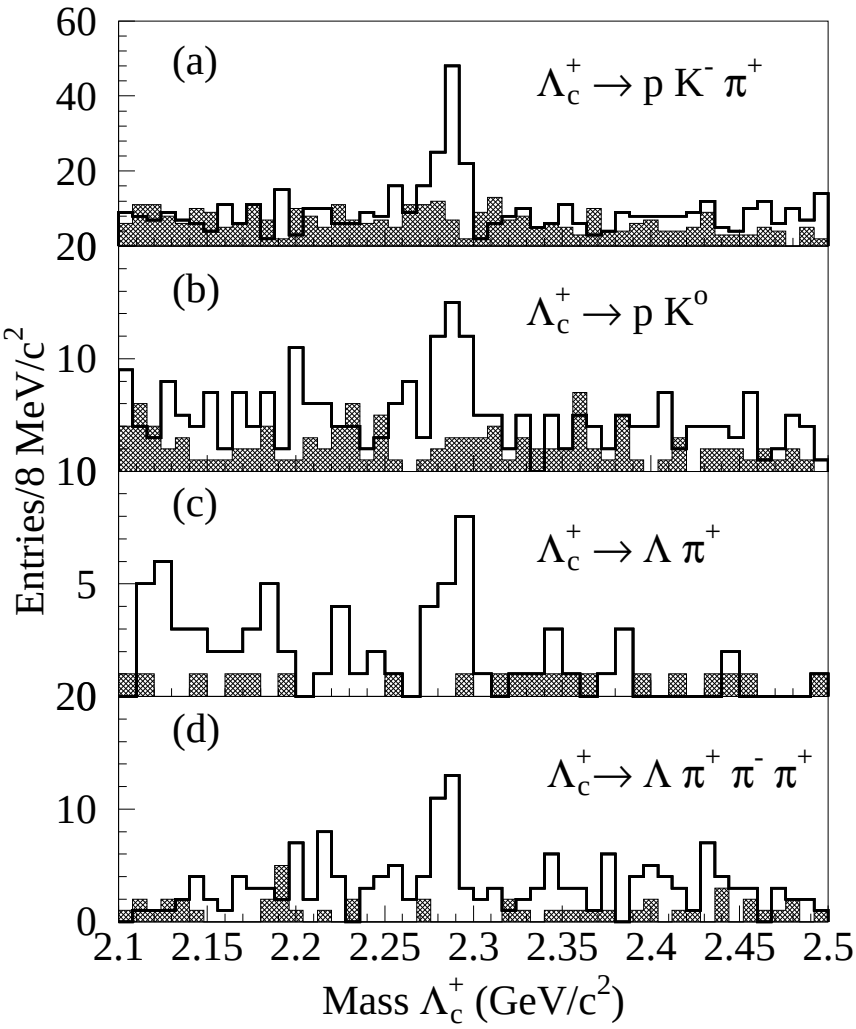

Figure 3: Invariant mass of the selected combinations of (a) $pK^-\pi^+$, (b) pK^0, (c) $\Lambda\pi^+$ and (d) $\Lambda\pi^+\pi^+\pi^-$ for the right-sign $\Lambda_c^+\ell^-$ combinations. The shaded plots show the corresponding wrong-sign $\Lambda_c^+\ell^+$ combinations.

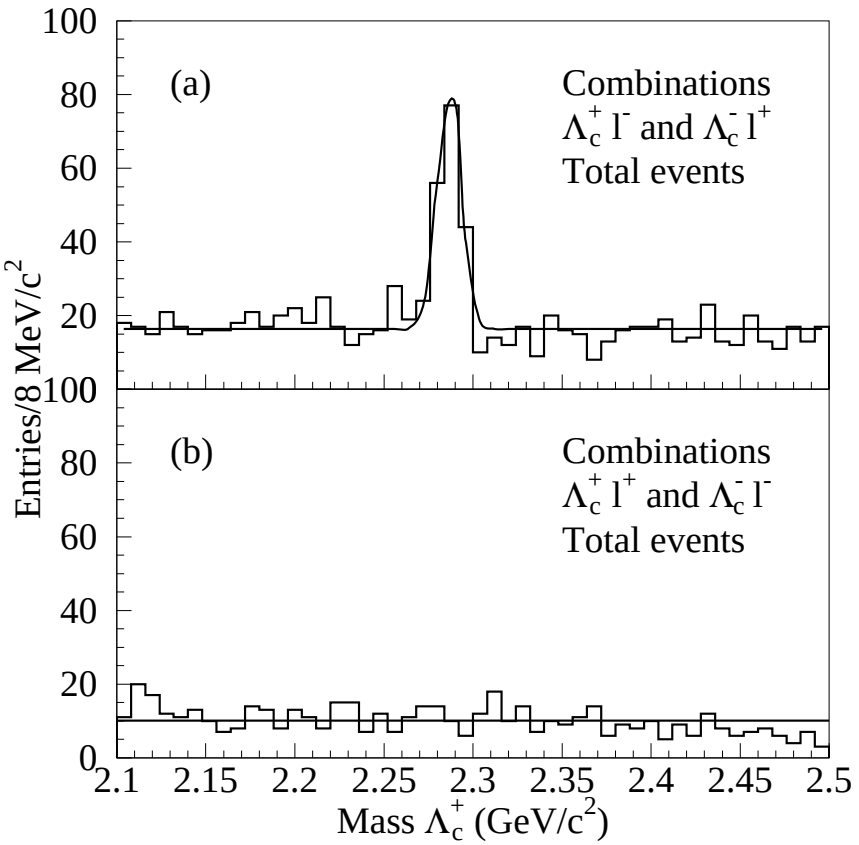

Figure 4: Invariant mass distribution of Λ_c^+ candidates associated to leptons in the four Λ_c^+ decay modes for the right-sign (a) and the wrong-sign (b) $\Lambda_c\ell$ combinations.

Decay Channel	Candidates	Background fraction (%)	mass resolution σ (MeV/c^2)
$\Lambda_c^+ \to pK^-\pi^+$	103	27 ± 2	6.9
$\Lambda_c^+ \to p\bar{K}^0$	35	29 ± 3	8.1
$\Lambda_c^+ \to \Lambda\pi^+$	18	39 ± 4	9.2
$\Lambda_c^+ \to \Lambda\pi^+\pi^+\pi^-$	37	31 ± 3	5.1
Total	193	29 ± 1	–

Table 4: The number of $\Lambda_c^+\ell^-$ candidates and the fraction of combinatorial background within $\pm 2\sigma$ of the nominal Λ_c^+ mass in the four Λ_c^+ decay modes after all requirements. The value of σ, estimated from the Monte Carlo, is also reported for each channel.

4.2 Decay proper time and lifetime fit

For each Λ_b candidate, the proper time is obtained from the Λ_b decay length l, the Λ_b momentum p, and the Λ_b mass M by the formula:

$$t(\Lambda_b) = \frac{lM}{p}.$$

The Λ_b decay length is measured in three dimensions by projecting the vector joining the interaction point and the Λ_b decay vertex onto the Λ_b flight direction as estimated from the $\Lambda_c^+\ell^-$ combination. The typical resolution of the Λ_c^+ and the Λ_b decay vertices along their directions of flight are 330 μm and 180 μm respectively. For each event, the error on the Λ_b decay length is calculated from the track trajectory errors. To estimate the accuracy of these errors, a distribution of the difference between the measured and the true decay length, divided by its uncertainty, is built for Monte Carlo events. From a double Gaussian fit to these distributions, two different correction factors on the measured decay length error have been estimated for each channel. The correction factors have been further modified by a scale factor that takes into account differences in the decay length resolution between data and Monte Carlo.

The Λ_b momentum is determined event by event from the measured $\Lambda_c^+\ell^-$ energy and the reconstructed neutrino energy in the $\Lambda_c^+\ell^-$ hemisphere with the same technique as described in Ref. [20]. A resolution function, κ, is defined as the ratio of reconstructed to true momentum of the Λ_b, in order to take into account the uncertainty on the Λ_b momentum reconstruction. It is obtained for each channel from Monte Carlo simulation and is used to fit the data. For the Λ_b mass, the world average is used: $\mathrm{M}(\Lambda_b) = 5621 \pm 5$ MeV/c^2 [21].

The Λ_b lifetime is extracted from a simultaneous unbinned maximum likelihood fit to the proper time distribution of the four $\Lambda_c^+\ell^-$ event samples shown in Table 4. The fitting technique is similar to that described in [20]. The fraction of combinatorial background events differs among the four Λ_c^+ decay modes; it is 29% on average. The parametrisation for the background in each $\Lambda_c^+\ell^-$ sample is taken from a fit to right-sign events from side bands (more than 4σ outside the nominal Λ_c^+ mass) and wrong-sign events.

Fig. 5 shows the result of the simultaneous fit of the Λ_b signal and combinatorial background events. The fitted Λ_b lifetime is

$$\tau(\Lambda_b) \;=\; 1.21\,^{+0.13}_{-0.12}\ \mathrm{ps},$$

where the quoted error is statistical only.

4.3 Systematic errors

The sources of systematic error are summarized in Table 5. The increase in statistics with respect to the previous published analysis allows the reduction of the systematic errors due to the fraction and shape of the combinatorial background. By varying the background shape in the fit, a systematic uncertainty of ± 0.022 ps is estimated.

The fraction of combinatorial background events in the peak has been varied within its statistical error. This leads to a change in the fitted Λ_b lifetime of ± 0.003 ps.

The contribution of the background due to processes (2), (3) and (5) of Section 3 is estimated using a dedicated Monte Carlo sample to be (4 ± 4) % of the $\Lambda_c^+\ell^-$ candidates. Adding a lifetime component to the background probability density function to reproduce the possible lifetime bias

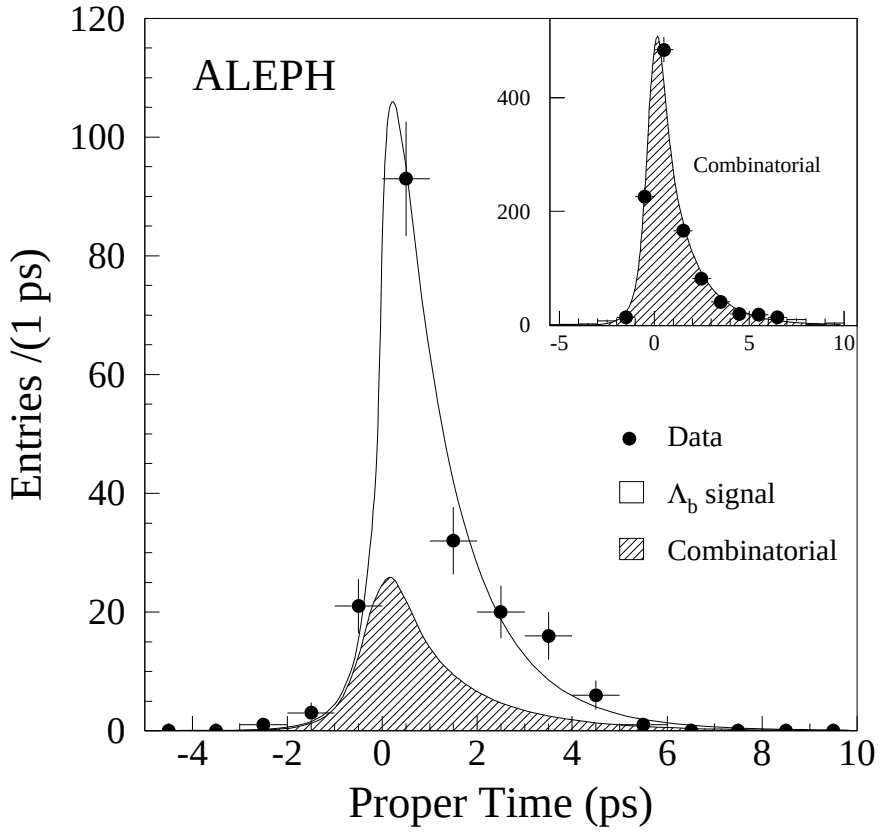

Figure 5: The proper-time distribution of the Λ_b candidates in the $\Lambda_c^+\ell^-$ sample. The shaded area corresponds to the proper-time distribution of the combinatorial background. The solid curve is the result of the maximum likelihood fit. The inset shows the proper time distribution of the combinatorial background from wrong-sign and right-sign sidebands events with the fitted parametrisation.

Source	Uncertainty (ps)
Combinatorial background shape	± 0.022
Physics background (4 ± 4 %)	∓ 0.017
Resolution function	± 0.011
Λ_b decay model (20% $\pm$20% four-body)	∓ 0.011
b fragmentation ($\langle x_{\Lambda_b} \rangle = 0.715 \pm 0.030$)	∓ 0.008
Λ_b polarization ($\mathcal{P}_{\Lambda_b} = -23^{+25}_{-21}$%)	$^{+0.004}_{-0.003}$
E_ν calibration	± 0.005
Combinatorial background fraction	± 0.003
Λ_b mass (5621 ± 5) MeV/c^2	± 0.001
Total	± 0.033

Table 5: Sources of systematic uncertainty on the Λ_b lifetime

introduced by these events decreases the fitted Λ_b lifetime by 0.017 ps. The central value of the fitted Λ_b lifetime has been corrected by this amount.

To estimate the systematic error due to the decay length resolution function an alternative parametrisation has been used. Varying the widths and the relative fractions of the two Gaussians used to describe this function by 20%, the Λ_b lifetime changes by ± 0.011 ps.

The momentum resolution function depends on several Monte Carlo parameters such as the fragmentation scheme [17], the Λ_b polarization [16] and the Λ_b decay model. The systematic uncertainty on the Λ_b lifetime due to the polarization is $^{+0.004}_{-0.003}$ ps while the uncertainty on the fragmentation function affects the measurement by 0.008 ps. To estimate the effect of the semileptonic decay model assumption on the Λ_b lifetime, the possibility of having a final state of four or more particles has been taken into account. Introducing a 20 ± 20% fraction of four body semileptonic Λ_b decays ($\Lambda_b \to \Lambda_c^+ \, l^- \bar{\nu} \pi^0$ or ρ^0) in the Monte Carlo, the measured Λ_b lifetime changes by -0.011 ∓ 0.011 ps. A correction of -0.011 ps is therefore added to the central value of the fitted Λ_b lifetime. To estimate the systematic error due to neutrino energy reconstruction error, the relative proportion of events in the tail of the κ distribution is varied by 20%. This leads to an uncertainty of ± 0.005 ps in the Λ_b lifetime.

The variation of the fitted Λ_b lifetime due to the uncertainty on the Λ_b mass is ± 0.001 ps.

Combining the systematic errors from these sources, the total systematic error is ± 0.033 ps. The final value for the lifetime is

$$\tau(\Lambda_b) \; = \; 1.18 \, ^{+0.13}_{-0.12} \pm 0.03 \text{ ps},$$

which supersedes the previous ALEPH value [6].

5 Λ_b Lifetime from $\Lambda\ell^+\ell^-$ combinations

A third sample of Λ_b baryons is reconstructed using $\Lambda_c^+\ell^-$ combinations with semileptonic decay of the Λ_c^+:

$$\begin{aligned}\Lambda_b \;\longrightarrow\; & \Lambda_c^+\ell_1^-\overline{\nu}X \\ & \hookrightarrow \Lambda\ell_2^+\nu X \\ & \quad\hookrightarrow p\pi^- ,\end{aligned}$$

i.e. a double semileptonic decay. A similar technique was used in the ALEPH measurement of the B_s^0 lifetime using $\phi\ell^+\ell^-$ combinations [22].

5.1 Sources of $\Lambda\ell^+\ell^-$ combinations

Five sources of $\Lambda\ell^+\ell^-$ combinations are considered. They are:

(A) $\Lambda_b \to \Lambda_c^+\ell_1^-\overline{\nu}X, \quad \Lambda_c^+ \to \Lambda\ell_2^+\nu X$

(B) $\Xi_b^{-/0} \to \Xi_c^{0/+}\ell_1^-\overline{\nu}X, \quad \Xi_c^{0/+} \to \Xi^{-/0}\ell_2^+\nu X, \quad \Xi^{-/0} \to \Lambda\pi^{-/0}$

(C) $B \to D\ell_1^-\overline{\nu}X, \quad D \to \ell_2^+\nu X \;+\;$ fragmentation Λ

(D) $B \to D\ell_1^-\overline{\nu}X, \quad D \to \ell_2^+\nu X \;+\;$ combinatorial Λ

(E) $B \to J/\psi X, \quad J/\psi \to \ell_1^-\ell_2^+ \;+\; \Lambda$

The first is the signal process, used to measure the lifetime of the Λ_b. The second process is due to the same decay of the strange b baryon, and differs from the signal process only in the presence of an extra pion. The third source is due to two leptons from double semileptonic b quark decay ($b \to c\ell_1^-\overline{\nu}$, $c \to s\ell_2^+\nu$) combined with a Λ produced in the fragmentation process. Random track combinations that sum to the Λ mass combined with the same double semileptonic b decay form the fourth source. Decays of the J/ψ, the fifth source, are specifically rejected and do not enter the sample. Hadrons misidentified as leptons were found to contribute negligibly as the first lepton. They contribute slightly for ℓ_2 and are included in background sources (C) and (D).

5.2 Selection criteria

Lambda baryons are selected using the algorithm described in Section 3, with the minimum momentum lowered to 2 GeV/c, and the minimum decay radius to 1 cm. The p and π^- are identified via their ionization energy loss in the TPC, when such a measurement is available. Proton candidates are required to satisfy $\chi_p + \chi_\pi < 0$ where χ_i is the normalized dE/dx under hypothesis i. The π^- candidate's ionization is required to lie within three standard deviations of expectation.

The proton and pion candidates are fitted to a common vertex and rejected if the probability of such a vertex is less than 10^{-4}, which reduces the combinatorial background. The $p\pi^-$ invariant mass is required to lie within two standard deviations of the nominal Λ mass, taking into account the momentum dependence as in Section 3.

Electron candidates for ℓ_1 are required to have at least 2 GeV/c of momentum. The first lepton is also required to have a transverse momentum with respect to its nearest jet of at least 1 GeV/c. The second lepton, coming from the charm baryon decay, is expected to have

a softer momentum spectrum. Electron candidates for ℓ_2 of at least 2 GeV/c must pass the same identification requirements as for ℓ_1 . However, electrons of between 1 and 2 GeV/c are accepted if ionization energy loss information is available and is incompatible with the proton hypothesis by at least two standard deviations, as in [22]. From simulation this results in a 17% relative increase in selection efficiency for this decay mode. Muon candidates for both ℓ_1 and ℓ_2 are required to have at least 3 GeV/c of momentum.

To ensure accurate decay length reconstruction, the two leptons are required to have at least one VDET space point measurement each. They must form a common vertex with probability greater than 1%; this helps to eliminate the background due to processes (C) and (D) and leptons from hadrons decaying in flight. The lepton pair is also required to have invariant mass greater than 100 MeV/c^2 and outside the range 3.0 – 3.15 GeV/c^2, to avoid photon conversions and J/ψ decays.

The invariant mass of the Λ and ℓ_2^+ is required to be less than 2.3 GeV/c^2, and that of the two leptons and the Λ greater than 2.3 GeV/c^2. This ordering of the two leptons allows a comparison of their charge with the baryon number of the lambda. Requiring a right-sign combination then reduces the combinatorial background by half. In addition, the $\Lambda\ell_1^-\ell_2^+$ invariant mass is required to be less than 5.6 GeV/c^2.

As the signal decay has low multiplicity, candidate hemispheres are required to have at most nine charged or neutral energy flow [10] objects with $\cos\theta > 0.95$ with respect to ℓ_1. This requirement eliminates 50% of the remaining background events while retaining 90% of the signal events, according to simulation.

Double semileptonic Ξ_b decays, (B), differ from the signal process only in the presence of an additional π from the decay $\Xi \to \Lambda\pi$ at the end of the decay chain. In order to suppress this physics background, a search is performed for the final pion. If one is found that forms an invariant mass with the Λ within 15 MeV/c^2 of the Ξ^- mass (50 MeV/c^2 for the π^0 from Ξ^0), the event is rejected. For the charged pion, this search eliminates 75% of the background process while retaining 94% of the signal, according to simulation. The neutral case is more difficult, 26% of these background events are found and rejected with 97% of signal decays retained.

5.3 Effective variable selection

To obtain the best selection efficiency after this preselection, an effective variable technique is used to combine variables to discriminate between background and signal processes. This technique has been used in previous ALEPH analyses and is explained in detail there [23, 24].

Only kinematic observables are used in constructing the effective variable, $X_{\rm eff}$. Table 6 lists the quantities used with the signal/background separation of each. The separation power of an observable x is defined in [23]; it is one for full separation of signal and background, zero for complete overlap. For comparison, the separation of two Gaussians of unit width one standard deviation apart is 0.31.

The distribution of this estimator for signal and for the sum of the three background processes after the preselection has been applied is shown in Fig. 6. Events lying below 0.8 are selected. This requirement has an efficiency of approximately 75% for signal and 55% for the three backgrounds together, 30% for the fragmentation Λ background. The total reconstruction efficiency for the signal process is increased by approximately 15% (relative) over a comparable set of requirements on the individual variables that would result in a sample of similar purity.

Observable	S/B Separation	Observable	S/B Separation
$p(\Lambda)$	0.34	$p(\Lambda\ell_2^+)$	0.22
$p(\Lambda\ell_1^-\ell_2^+)$	0.32	$p(\ell_1^-\ell_2^+)$	0.22
rapidity(Λ)	0.32	$\cos\theta_1^*$	0.21
$m(\Lambda\ell_2^+)$	0.30	$\cos\theta_2^*$	0.20
$p_\perp(\ell_1^-)$	0.30	$m(\ell_1^-\ell_2^+)$	0.18
$m(\Lambda\ell_1^-\ell_2^+)$	0.23		

Table 6: Kinematic quantities used in the effective variable selection of $\Lambda\ell_1^-\ell_2^+$ candidates and the separation between signal and background processes each provides. Perfect separation is 1 on this scale. The angle θ_1^* is the decay angle of ℓ_1^- in the $\Lambda\ell_1^-\ell_2^+$ rest frame; θ_2^* is the angle of ℓ_2^+ in the $\Lambda\ell_2^+$ rest frame.

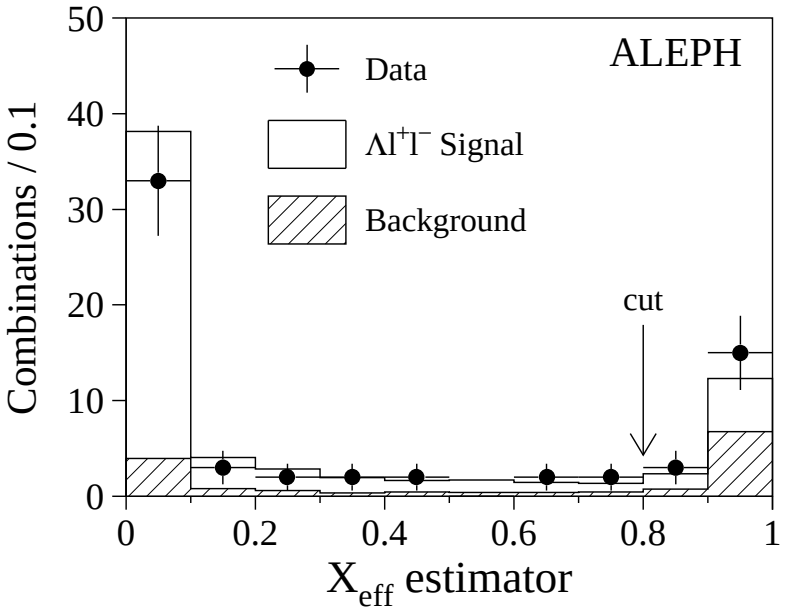

Figure 6: Distribution of X_{eff} for signal and background processes after the preselection. Events with $X_{eff} < 0.8$ are accepted in the analysis.

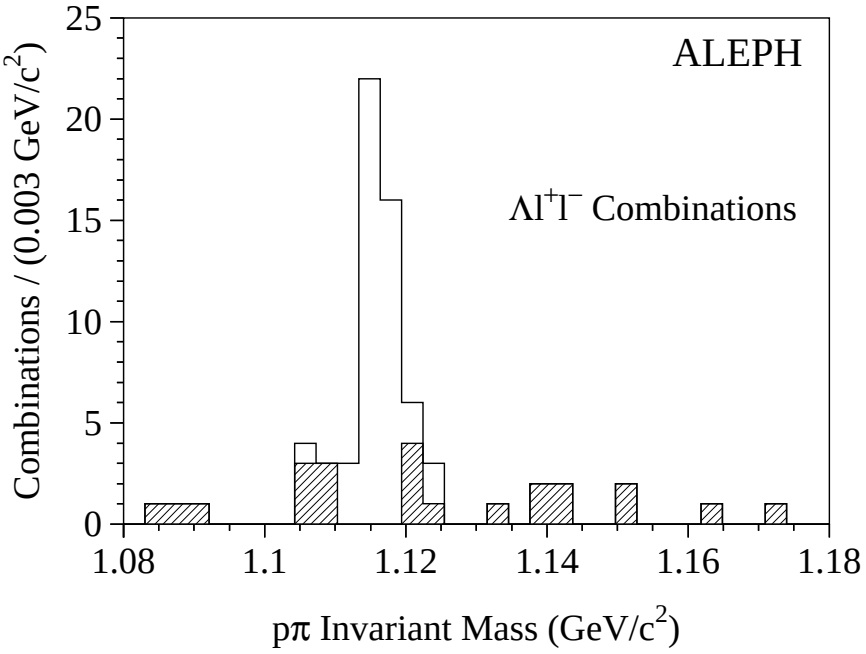

Figure 7: The $p\pi^-$ invariant mass distribution of the $\Lambda\ell^+\ell^-$ candidate events. The shading indicates the events lying outside the momentum-dependent mass window.

5.4 Sample composition

The above requirements select 46 events in the data. The $p\pi^-$ invariant mass of these candidates is shown in Fig. 7, with the events outside the variable mass window shaded.

The contributions of the three background processes are calculated from their production rates, estimated below, and the efficiency with which they pass the above selection criteria, estimated from Monte Carlo simulation. All remaining events are ascribed to the Λ_b signal.

The Ξ_b baryon has been observed and its lifetime measured by ALEPH and DELPHI [24, 25]. The combined value for the production rate of Ξ_b in $Z \to b\overline{b}$ decay is $\mathrm{Br}(b \to \Xi_b) \cdot \mathrm{Br}(\Xi_b \to \Xi^-\ell^-\overline{\nu}X) = (5.5 \pm 1.2) \times 10^{-4}$. Assuming the intermediate state includes Ξ_c, an estimate of the production rate of the double-semileptonic final state is possible. This requires two unmeasured quantities, $\mathrm{Br}(\Xi_c^0 \to \Xi^-\ell^+X)$ and $\mathrm{Br}(\Xi_c^0 \to \Xi^-X)$. Assuming equality of semileptonic partial widths, the first may be inferred from the measured rate for $\mathrm{Br}(\Lambda_c^+ \to \Lambda\ell^+X)$ and the lifetimes $\tau(\Xi_c^0)$ and $\tau(\Lambda_c^+)$ [1]. Due to the additional strange quark, $\mathrm{Br}(\Xi_c^0 \to \Xi^-X)$ should be larger than the corresponding value for Λ_c^+, $\mathrm{Br}(\Lambda_c^+ \to \Lambda X) = 35 \pm 11\%$. It is taken to be $68 \pm 32\%$, midway between the Λ_c^+ value and unity, with an error to span the range. Using these and other, known values from [1], the product branching fraction of Ξ_b^- to the final state of interest is

$$\mathrm{Br}(b \to \Xi_b^-) \cdot \mathrm{Br}(\Xi_b^- \to \Xi_c^0\ell^-\overline{\nu}X) \cdot \mathrm{Br}(\Xi_c^0 \to \Xi^-\ell^+X) = (2.4^{+2.4}_{-1.3}) \times 10^{-5} \ .$$

A similar calculation for the neutral strange b baryon yields $(8.6^{+8.6}_{-4.7}) \times 10^{-5}$. From Monte Carlo simulation, the efficiencies to pass the selection criteria are $0.45 \pm 0.12\%$ and $2.8 \pm 0.3\%$ for the charged and neutral cases, respectively. The number of expected events in the sample is

Source	N events	Fraction (%)	Lifetime (ps)
Ξ_b	$2.7\ ^{+2.6}_{-1.4}$	$5.9\ ^{+5.7}_{-3.1}$	$1.39\ ^{+0.35}_{-0.27}$
Fragmentation Λ	1.6 ± 0.4	3.4 ± 0.8	$1.89\ ^{+0.39}_{-0.31}$
Combinatorial Λ	2.2 ± 1.0	4.7 ± 2.3	$2.45\ ^{+0.48}_{-0.38}$
Λ_b	$39.5\ ^{+1.8}_{-2.8}$	$86.0\ ^{+3.9}_{-6.2}$	–

Table 7: Source fractions and lifetimes used in the likelihood fit to the Λ_b lifetime in the $\Lambda\ell^+\ell^-$ decay mode. Derivations are given in the text.

$0.11^{+0.11}_{-0.07}$ from Ξ_b^- decays and $2.6^{+2.6}_{-1.4}$ from Ξ_b^0. The contributions are combined.

The fragmentation Λ background contribution is estimated from simulation. A total of 1.6 ± 0.4 events are predicted.

The contribution of the combinatorial Λ background is estimated from a fit to the data, using the $p\pi^-$ invariant mass sidebands. The data are subdivided into momentum bins and fitted with a Gaussian for the signal and a flat background shape. In total, 2.2 ± 1.0 events are expected.

The estimated composition of the $\Lambda\ell^+\ell^-$ sample is summarized in Table 7.

5.5 Estimate of the Λ_b proper decay time and likelihood fit to the lifetime

As in the $\Lambda_c^+\ell^-$ analysis described in Section 4, the proper time of each Λ_b candidate is inferred from measurements of its momentum and decay length. The mass of the Λ_b used is 5621 ± 5 MeV/c^2 [21].

As the Λ decays well outside the vertex detector, the decay length of the Λ_b is estimated as the three-dimensional separation between the vertex formed by the two lepton tracks and that of the primary interaction point, projected onto the flight direction of the $\Lambda\ell^+\ell^-$ system. Due to the Λ_c^+ lifetime, this causes a slight overestimate of the decay length which is taken into account in the lifetime fit.

This decay length estimation method has a core resolution of approximately $270 \pm 40\,\mu$m for 72% of the events and $1010 \pm 110\,\mu$m for the remainder. These values are taken from simulation and have been scaled by 1.08 ± 0.13, the observed difference in resolution between lepton-hadron vertices of negative decay length fitted in data and in the ALEPH Monte Carlo. A similar scaling was performed in [22]. The offset due to the Λ_c^+ lifetime is $52\,\mu$m.

The momentum of the Λ_b is calculated from the measured momentum sum of the $\Lambda\ell^+\ell^-$ system and an estimate of the momentum taken away by the two neutrinos. This missing energy technique is identical to that used in the $\Lambda_c^+\ell^-$ analysis described in Section 4. The κ distribution has a mean of 0.96 and an RMS of 17% for this decay mode.

The lifetime is measured with an unbinned maximum likelihood fit to the proper time distribution of the 46 $\Lambda\ell^+\ell^-$ events. The likelihood is similar to that described in Section 4. In addition to the signal process, there are components for the three backgrounds: processes (B), (C) and (D), whose assumed contributions to the sample were described above and summarized in Table 7. The other inputs to the likelihood fit are described here.

The average of the ALEPH and DELPHI measurements of the Ξ_b baryon lifetime [24, 25] is $1.39^{+0.35}_{-0.27}$ ps. In order to use this lifetime in the fit, a κ distribution independent of that for the

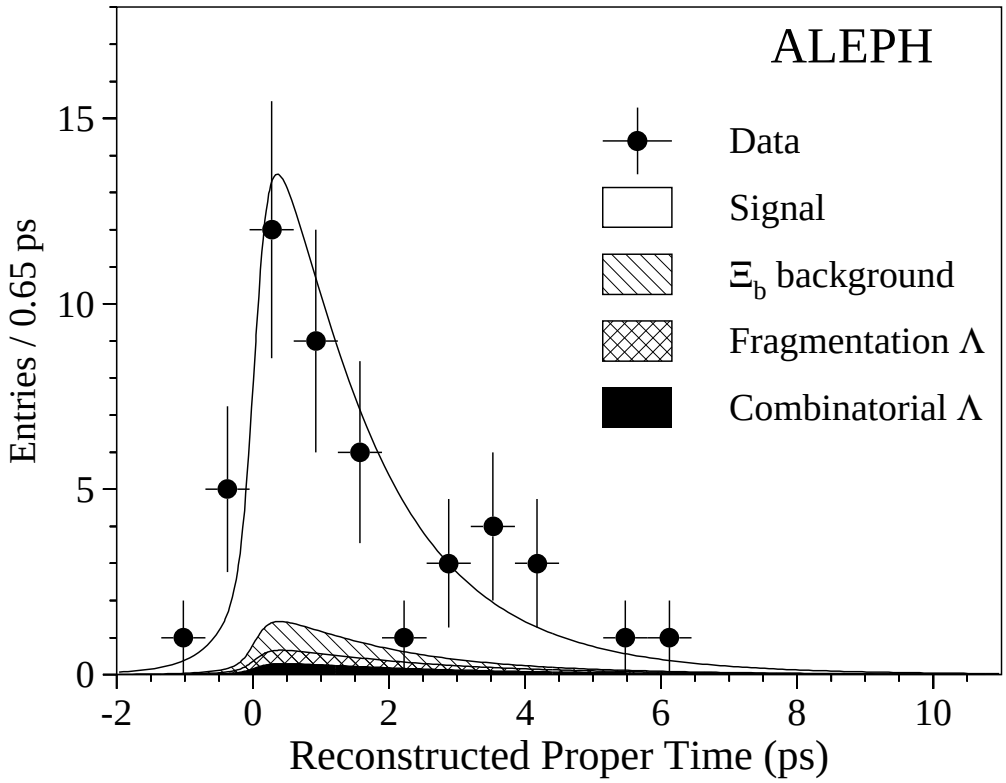

Figure 8: Fit to the proper time distribution of the 46 candidates reconstructed in the $\Lambda\ell^+\ell^-$ decay mode.

signal process is used, taken from simulation. It has a mean slightly lower than that for the signal process due to the missing pion.

The fragmentation and combinatorial Λ backgrounds are assigned an effective lifetime in the likelihood. For the fragmentation case, this is fitted to the Monte Carlo. The value obtained (Table 7) is higher than the average b hadron lifetime due to the relatively low momentum of fragmentation Λ's. Additionally, the longer D lifetime creates a $\ell_1\ell_2$ vertex further from the B decay point than the Λ_c^+ does in the signal decay.

The effective lifetime of the combinatorial background is estimated from a fit to events in the upper sideband of the Λ mass spectrum in the data, $1.14 < \mathrm{M(p}\pi) < 1.18$ GeV/c^2. The selection criteria on the number of energy flow objects and $\mathrm{d}E/\mathrm{d}x$ were removed, selecting 36 events. The effective lifetime is higher than $\langle\tau_\mathrm{b}\rangle$ due to the underestimated momentum and overestimated decay length.

The result of the unbinned maximum likelihood fit to the 46 events observed in data is $\tau(\Lambda_\mathrm{b}) = 1.33^{+0.28}_{-0.23}$ ps. The quoted error is statistical in nature; the systematic uncertainties and corrections are described below. The proper time distribution of the data with the fit superimposed is shown in Fig. 8.

5.6 Systematic uncertainties and corrections

The systematic uncertainties considered are listed in Table 8 and described here.

- The background process fractions are varied by their uncertainties, changing the fitted lifetime by ∓ 0.023 ps. The combinatorial Λ fraction dominates.

Source	Correction (ps)	Uncertainty (ps)
Background fractions	–	∓ 0.023
Decay length resolution	–	∓ 0.021
Four-body decays ($20 \pm 20\%$ π^0/ρ^0)	-0.020	∓ 0.020
Background lifetimes	–	∓ 0.014
Fragmentation ($\langle x_b \rangle = 0.715 \pm 0.030$)	–	∓ 0.007
Λ_b polarization ($P_{\Lambda_b} = -23^{+25}_{-21}\%$)	-0.007	$^{+0.007}_{-0.006}$
$m(\Lambda_b) = 5.621 \pm 0.005$ GeV/c^2	–	± 0.001
Total	-0.027	± 0.041

Table 8: The systematic uncertainties and corrections of the measurement of $\tau(\Lambda_b)$ from $\Lambda\ell^+\ell^-$ combinations.

- The errors on the decay length resolution, including a 100% variation of the offset due to $\tau(\Lambda_c^+)$, result in a ∓ 0.021 ps variation in the fitted Λ_b lifetime.
- Allowing 20% of the signal decay process to be four-body decays, *i.e.* $\Lambda_b \to \Lambda_c^+ \ell^- \overline{\nu} \pi^0$ or ρ^0, the κ distribution shifts and results in a correction of the fitted lifetime of -0.020 ps. This contribution is varied by $\pm 100\%$.
- Varying the input lifetimes of the three background processes by their uncertainties results in a variation of ∓ 0.014 ps on the fitted lifetime. The uncertainty on $\tau(\Xi_b)$ contributes negligibly.
- The b quark fragmentation function is varied as in Section 3; that is, $\langle x_b \rangle = 0.715 \pm 0.030$, twice the uncertainty seen for B mesons. This causes a variation in the fitted lifetime of ∓ 0.007 ps.
- Using the Λ_b polarization measurement, a correction and uncertainty of $-0.007^{+0.007}_{-0.006}$ ps are observed.
- Finally, varying the measured value of the Λ_b mass by its errors results in an additional ± 0.001 ps systematic uncertainty on $\tau(\Lambda_b)$.

Summed in quadrature, these individual contributions give an estimated total systematic uncertainty on the Λ_b lifetime fitted in this channel of ± 0.041 ps. With the systematic corrections, the value for the lifetime is

$$\tau(\Lambda_b) \;=\; 1.30\,^{+0.26}_{-0.21} \pm 0.04 \text{ ps}.$$

6 Measurement of the Λ_b product branching fraction

Using the measured branching fractions for the five Λ_c^+ decay channels [1] and the reconstruction efficiencies from simulation, the excess of $\Lambda_c^+\ell^-$ and $\Lambda\ell^+\ell^-$ combinations can be used to estimate

the average product branching fraction $\mathrm{Br}(\mathrm{b} \to \Lambda_\mathrm{b}) \cdot \mathrm{Br}(\Lambda_\mathrm{b} \to \Lambda_\mathrm{c}^+ \ell^- \overline{\nu} \mathrm{X})$. Again, to increase the sample size and to avoid possible systematic effects due to an imperfect efficiency simulation, the requirements on the hits and vertex probability, used to insure precise decay length reconstruction, are removed. After subtracting the physical background contributions, estimated from simulation and measured rates [24, 25], the product branching fraction is calculated for each of the five Λ_c^+ decay channels (Table 9).

Decay channel	$\frac{\Gamma(\Lambda_\mathrm{c}^+ \to \mathrm{X})}{\Gamma(\Lambda_\mathrm{c}^+ \to \mathrm{pK}^- \pi^+)}$	Efficiency (%)	$\mathrm{Br}(\mathrm{b} \to \Lambda_\mathrm{b}) \cdot \mathrm{Br}(\Lambda_\mathrm{b} \to \Lambda_\mathrm{c}^+ \ell^- \overline{\nu} \mathrm{X})$
$\Lambda_\mathrm{c}^+ \to \mathrm{pK}^- \pi^+$	1.0	6.9 ± 0.1	$0.85 \pm 0.11 \pm 0.13\,\%$
$\Lambda_\mathrm{c}^+ \to \Lambda \pi^+ \pi^+ \pi^-$	0.66 ± 0.10	4.7 ± 0.1	$0.79 \pm 0.20 \pm 0.18\,\%$
$\Lambda_\mathrm{c}^+ \to \mathrm{p}\bar{\mathrm{K}}^0$	0.49 ± 0.07	10.1 ± 0.2	$0.96 \pm 0.23 \pm 0.21\,\%$
$\Lambda_\mathrm{c}^+ \to \Lambda \pi^+$	0.18 ± 0.03	8.2 ± 0.2	$0.74 \pm 0.28 \pm 0.18\,\%$
$\Lambda_\mathrm{c}^+ \to \Lambda \ell^+ \nu$	0.52 ± 0.09	11.6 ± 0.3	$0.92 \pm 0.14 \pm 0.22\,\%$
Average	–	–	$0.86 \pm 0.07 \pm 0.14\,\%$

Table 9: Measurements of the product branching fraction in each of the five reconstructed decay modes of the Λ_c^+. Reconstruction efficiencies are obtained from simulation; the relative branching fractions are from Ref. [1]. The value of $\mathrm{Br}(\Lambda_\mathrm{c}^+ \to \mathrm{pK}^- \pi^+)$ used is $4.4 \pm 0.6\,\%$.

The measured rate, averaged over the electron and muon modes, is

$$\mathrm{Br}(\mathrm{b} \to \Lambda_\mathrm{b}) \cdot \mathrm{Br}(\Lambda_\mathrm{b} \to \Lambda_\mathrm{c}^+ \ell^- \overline{\nu} \mathrm{X}) \;=\; (0.86 \pm 0.07(\mathrm{stat}) \pm 0.14(\mathrm{syst}))\,\% \; .$$

The systematic uncertainty due to $\mathrm{Br}(\Lambda_\mathrm{c}^+ \to \mathrm{pK}^- \pi^+)$ is $\mp 0.12\,\%$. The second largest contribution to the systematic error, $\mp 0.04\,\%$, is due to the other branching fractions, that is, $\mathrm{R_b}$ and the relative branching fractions to each final state. The uncertainties on the levels of physical and combinatorial background contribute $\mp 0.04\,\%$ and $\mp 0.02\,\%$, respectively. The uncertainties on the selection efficiencies have a negligible effect.

7 Conclusion

In a total of approximately 4 million hadronic Z decays collected with the ALEPH detector between 1991 and 1995, the lifetime of the b baryon is measured with three independent methods. Semileptonic b baryon decays are selected using $\Lambda\ell$ correlations. The b baryon lifetime is measured from a maximum likelihood fit to the impact parameter distribution of candidate lepton tracks in this sample. The result is $\tau(\mathrm{b\ baryon}) = 1.20 \pm 0.08(\mathrm{stat}) \pm 0.06(\mathrm{syst})$ ps. From the observed yield of $\Lambda\ell^-$ and $\Lambda\ell^+$ combinations, the product branching ratio

$$\mathrm{Br}(\mathrm{b} \to \Lambda_\mathrm{b}) \cdot \mathrm{Br}(\Lambda_\mathrm{b} \to \Lambda \ell^- \overline{\nu} \mathrm{X}) \;=\; (0.326 \pm 0.016(\mathrm{stat}) \pm 0.039(\mathrm{syst}))\,\%$$

is measured, averaged over electrons and muons.

A maximum likelihood fit to the proper decay time distribution of 193 $\Lambda_\mathrm{c}^+ \ell^-$ combinations gives a value for the Λ_b lifetime of $\tau(\Lambda_\mathrm{b}) = 1.18\,^{+0.13}_{-0.12}(\mathrm{stat}) \pm 0.03(\mathrm{syst})$ ps.

A third sample of Λ_b's is reconstructed in the $\Lambda\ell^+\ell^-$ decay mode. From a maximum likelihood fit to the proper decay time distribution of this sample, the lifetime of the Λ_b is $\tau(\Lambda_b) = 1.30\,^{+0.26}_{-0.21}(\mathrm{stat}) \pm 0.04(\mathrm{syst})$ ps.

From the yield of the five decay modes comprising the $\Lambda_c^+\ell^-$ and $\Lambda\ell^+\ell^-$ samples, the product branching fraction of the Λ_b is measured. It is

$$\mathrm{Br}(b \to \Lambda_b) \cdot \mathrm{Br}(\Lambda_b \to \Lambda_c^+ \ell^- \overline{\nu} X) \;=\; (0.86 \pm 0.07(\mathrm{stat}) \pm 0.14(\mathrm{syst}))\,\% \;,$$

again averaged over electrons and muons.

As the second and third methods are independent and measure the lifetime of the Λ_b and not of b baryons in general, they can be averaged directly. The result is:

$$\tau(\Lambda_b) \;=\; 1.21 \pm 0.11 \text{ ps.}$$

Since the relative contribution of various b baryon species in the $\Lambda\ell^-$ sample is not well known and depends on their relative production rate and lifetime, there is no *a priori* prescription for averaging all the lifetime measurements described above. However, assuming that the Λ_b is the dominant source of b baryons produced at the Z resonance and the differences among the b baryon lifetimes (Λ_b , Ξ_b , Ω_b) are small, the b baryon and Λ_b measurements can be averaged. In order to have three statistically independent samples, 32 events in the $\Lambda\ell^-$ sample are removed (14 events are in common with the $\Lambda_c^+\ell^-$ sample and 18 are in common with the $\Lambda\ell^+\ell^-$ sample). The lifetime fit of the remaining 1031 $\Lambda\ell^-$ combinations yields $\tau(\text{b baryon}) = 1.22 \pm 0.08 \pm 0.06$ ps. The resulting average, taking into account the correlated systematic uncertainties, is

$$\tau(\text{b baryon}) \;=\; 1.21 \pm 0.08 \text{ ps.}$$

This value can be compared with the most recent measurements of the b baryon lifetime [26] and with the world average of the B_d^0 meson lifetime [1] of 1.56 ± 0.06 ps. The ratio of the lifetimes of Λ_b and B^0 hadrons is 0.78 ± 0.06, significantly smaller than the theoretical predictions [2, 3].

Acknowledgements

We thank our colleagues in the CERN accelerator divisions for the successful operation of the LEP storage ring. We also thank the engineers and technicians in all our institutions for their support in constructing and operating ALEPH. Those of us from non-member countries thank CERN for its hospitality.

References

[1] Particle Data Group, R.M. Barnett *et al.*, Phys. Rev. **D54** (1996) 1.

[2] I. Bigi *et al.*, Non-leptonic Decays of Beauty Hadrons - From Phenomenology to Theory, in "B decays", second edition. Singapore: World Scientific.

[3] M. Neubert and C.T. Sachrajda, Nucl. Phys. **B 483**, 339 (1987);
M. Neubert, "Theory of Beauty Lifetimes", CERN-TH/97-148.

[4] ALEPH Collaboration, Phys. Lett. **B 278** (1992) 209;
OPAL Collaboration, Phys. Lett. **B 281** (1992) 394;
DELPHI Collaboration, Phys. Lett. **B 311** (1993) 379.

[5] ALEPH Collaboration, Phys. Lett. **B 294** (1992) 145.

[6] ALEPH Collaboration, Phys. Lett. **B 357** (1995) 685.

[7] ALEPH Collaboration, Phys. Lett. **B 359** (1995) 236.

[8] ALEPH Collaboration, Nucl. Instrum. Methods **A 294** (1990) 121.

[9] B. Mours *et al.*, Nucl. Instrum. Methods **A 379** (1996) 101.

[10] ALEPH Collaboration, Nucl. Instrum. Methods **A 360** (1995) 481.

[11] ALEPH Collaboration, Z. Phys. **C 60** (1993) 71.

[12] ALEPH Collaboration, Z. Phys. **C 64** (1994) 361.

[13] T. Sjostrand, Comp. Phys. Comm. **82** (1994) 74.

[14] ALEPH Collaboration, Z. Phys. **C 62** (1994) 179.

[15] ALEPH Collaboration, Phys. Lett. **B 369** (1996) 151.

[16] ALEPH Collaboration, Phys. Lett. **B 365** (1996) 437.

[17] C. Peterson et al., Phys. Rev. **D27** (1983) 105.

[18] ALEPH Collaboration, Phys. Lett. **B 357** (1995) 699.

[19] ALEPH Collaboration, preprint CERN-PPE/97-018, "A Measurement of R_b using Mutually Exclusive Tags", to be published in Phys. Lett. **B**.

[20] ALEPH Collaboration, Phys. Lett. **B 322** (1994) 275.

[21] ALEPH Collaboration, Phys. Lett. **B 380** (1996) 442;
CDF Collaboration, Phys. Rev. **D55** (1997) 1142.

[22] ALEPH Collaboration, Phys. Lett. **B 361** (1995) 221.

[23] ALEPH Collaboration, Phys. Lett. **B 377** (1996) 205.

[24] ALEPH Collaboration, Phys. Lett. **B 384** (1996) 449.

[25] DELPHI Collaboration, Z. Phys. **C 68** (1995) 541.

[26] OPAL Collaboration, Z. Phys. **C 69** (1996) 195;
DELPHI Collaboration, Z. Phys. **C 71** (1996) 199.